

Effect of substitution of Mn with Fe or Cr in Heusler alloy of Co_2MnSn

This article has been downloaded from IOPscience. Please scroll down to see the full text article.

2005 J. Phys.: Condens. Matter 17 6653

(<http://iopscience.iop.org/0953-8984/17/42/006>)

View [the table of contents for this issue](#), or go to the [journal homepage](#) for more

Download details:

IP Address: 129.252.86.83

The article was downloaded on 28/05/2010 at 06:34

Please note that [terms and conditions apply](#).

Effect of substitution of Mn with Fe or Cr in Heusler alloy of Co_2MnSn

W Zhang^{1,2}, N Jiko³, K Mibu^{1,4} and K Yoshimura²

¹ Research Center for Low Temperature and Materials Sciences, Kyoto University, Gokasho, Uji, Kyoto 611-0011, Japan

² Department of Chemistry, Graduate School of Science, Kyoto University, Sakyo-ku, Kyoto 606-8502, Japan

³ Institute for Chemical Research, Kyoto University, Gokasho, Uji, Kyoto 611-0011, Japan

E-mail: wzhang@kuchem.kyoto-u.ac.jp

Received 3 August 2005

Published 7 October 2005

Online at stacks.iop.org/JPhysCM/17/6653

Abstract

Crystallographic and magnetic properties of $\text{Co}_2\text{Mn}_{1-x}\text{Fe}_x\text{Sn}$ and $\text{Co}_2\text{Mn}_{1-y}\text{Cr}_y\text{Sn}$ Heusler alloys were studied using x-ray diffraction, scanning electron microscopy with energy dispersive x-ray analysis, magnetization measurements and Mössbauer spectroscopy. We found that the intermetallic compounds crystallize into a single phase with the $L2_1$ -type Heusler structure at the concentration of $0 \leq x \leq 0.5$ for $\text{Co}_2\text{Mn}_{1-x}\text{Fe}_x\text{Sn}$ and $0 \leq y \leq 0.3$ for $\text{Co}_2\text{Mn}_{1-y}\text{Cr}_y\text{Sn}$. The spontaneous magnetization increases when Mn is substituted with Fe and decreases when Mn is substituted with Cr. The values of hyperfine field at the Sn nuclear sites in $\text{Co}_2\text{Mn}_{1-x}\text{Fe}_x\text{Sn}$ and $\text{Co}_2\text{Mn}_{1-y}\text{Cr}_y\text{Sn}$ also increase or decrease in combination with the size of magnetization. These measurements suggest that the Slater–Pauling behaviour in half-metallic full-Heusler alloys provides a good description of the substitution effect of Mn with Fe or Cr.

1. Introduction

Since the discoveries of tunnelling magneto-resistance (TMR) in layered structures of magnetic metals and non-magnetic insulators [1, 2], a new field of spin electronics has been boosted up because of its applications for magnetic information storage [3]. The TMR ratio depends on the spin polarization (P) at the Fermi level of the magnetic materials as $\text{TMR} = 2P_1P_2/(1 - P_1P_2)$, where P_1 and P_2 are the conduction electrons' spin polarization for the two ferromagnetic metals in the layered tunnelling structures [4]. The recent excitement in Heusler alloys is triggered by the possibility that they are half-metallic ferromagnets, which present a gap in

⁴ Present address: Graduate School of Engineering, Nagoya Institute of Technology, Showa-ku, Nagoya 466-8555, Japan.

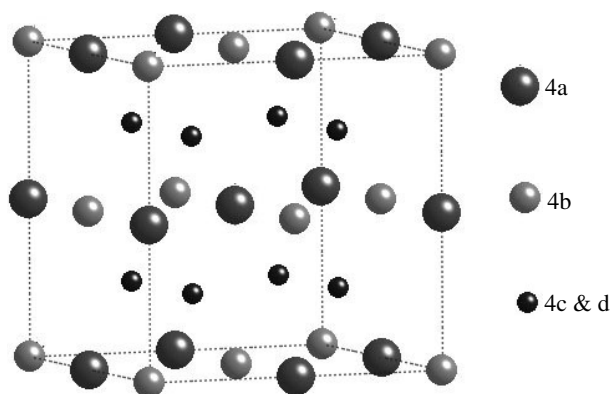


Figure 1. Co_2MnSn in the $L2_1$ -(Cu_2MnAl) type structure with $Fm\bar{3}m$ symmetry. The 4a and 4b sites are occupied by Mn and Sn respectively; the 4c and 4d sites by Co atoms.

the minority band and 100% spin polarized electrons ($P = 1$) in the Fermi level [5]. Inomata *et al* have demonstrated that a large TMR of 16% at room temperature was attained using $\text{Co}_2\text{Cr}_{1-x}\text{Fe}_x\text{Al}$ ($x = 0$ and 0.4) films [6]. Recently Kubota *et al* have observed TMR ratio at room temperature as high as 40% using Co–Mn–Al Heusler alloy [7].

Co_2MnSn Heusler alloy attracts attention because it is a ferromagnet with a high Curie temperature ($T_c \sim 830$ K) [8]. The neutron diffraction measurement by Webster showed that Co_2MnSn has a net moment of $5.08 \mu_B$ per formula and individual moments of $\sim 3.58 \mu_B$ and $\sim 0.75 \mu_B$ per Mn and Co atom, respectively [9].

As indicated in figure 1, Co_2MnSn has the $L2_1$ -(Cu_2MnAl) type structure. 4a and 4b sites are occupied by Mn and Sn respectively; 4c and 4d sites are occupied by Co atoms. Each Sn or Mn atom in the lattice of Co_2MnSn has eight Co atoms as the nearest neighbours and six Mn or Sn atoms as the next nearest neighbours, while each Co has four Mn and four Sn atoms as the first neighbours. In disordered structures, ions occupy sites other than those specified for the ordered structure. When the disorder occurs exclusively between Mn and Sn, the order parameter is expressed as $q = 2p - 1$, where p refers to the fraction of Mn atoms on their proper sites. When $p = 0.5$ or $q = 0$, the Mn–Sn disorder is the largest, i.e., the structure is alternatively described as a $B2$ -type structure.

Co_2MnSn contains ^{119}Sn atoms, which can be used to investigate magnetism through the Mössbauer effect [10–16]. Disorder between the Mn and Sn sites causes a distribution of the hyperfine fields (B_{hf}) at the Sn sites, which broadens the lines of Mössbauer spectrum. So, the width of the B_{hf} distribution is a measure of the extent of disorder in Co_2MnSn . The B_{hf} also give us information on magnetic moments of surrounding atoms.

Ishida *et al*, performing band-structure calculations for Co_2MnSn by the symmetrized augmented plane wave (SAPW) method, have shown that Mn is expected to carry a large magnetic moment whereas Co is expected to carry a small one [17]. According to the results of band calculations by Kübler *et al* the minority-spin-state densities at the Fermi energy nearly vanish and Co_2MnSn is half-metallic [18]. On the other hand, Picozzi *et al* indicated with *ab initio* calculations that there is finite spin-down density of states at the Fermi level instead of an absolute gap [19]. By using the full-potential screened Korringa–Kohn–Rostoker method, Galanakis *et al* [20] have shown that many of the Heusler alloys based on Co, Fe, Rh, and Ru have half-metallic character and follow a Slater–Pauling behaviour.

Inspired by these results, we started to investigate the Mn site substitution effect by Fe or Cr in Co_2MnSn . We prepared the intermetallic compounds of $\text{Co}_2\text{Mn}_{1-x}\text{Fe}_x\text{Sn}$

and Co₂Mn_{1-y}Cr_ySn by the arc melting method, and studied the substitution effect by structure analysis using x-ray diffraction, magnetization measurements, and ¹¹⁹Sn Mössbauer spectroscopy. The experimental methods are described in section 2 and the results are presented in section 3. The experimental results are compared with the predictions of current theories such as Slater–Pauling behaviour in Heusler alloys [20], and discussed in section 4. Finally, we summarize the results in section 5.

2. Experimental method

The alloys were prepared in the form of 10 g ingots by melting together a stoichiometric mixture of 4 N pure constituent metals in an argon arc furnace. The compositions of the samples were checked by scanning electron microscopy (SEM) with energy dispersive x-ray analysis (EDX). We found that the stoichiometry of the samples is accurate, and that the deviations from designed composition are less than 1%. For x-ray diffraction (XRD), magnetic analysis and Mössbauer effect measurements, the samples were ground into fine powder under the protection of organic solvent to prevent them from possible oxidization. All the samples are hard and brittle, so that they can be crushed readily in a hardened mortar.

For the structural investigation, XRD measurements were performed by the Debye–Scherrer method using Cu K α radiation at room temperature. Lattice parameters were determined from XRD data by means of the Wilson–Pike deviation function calculating method using (331), (420), and (422) reflections. The ratio of the Bragg reflection intensities, $I(111)/I(220)$, was used to estimate the extent of disorder in Co₂MnSn [21]. The structure with $Fm\bar{3}m$ symmetry gives rise to Bragg reflection from the (111) and (220) planes with nonzero structure factors:

$$F(111) = 4|(f_{4a} - f_{4b})^2 + (f_{4c} - f_{4d})^2|^{\frac{1}{2}}, \quad (1)$$

$$F(220) = 4|f_{4a} + f_{4b} + f_{4c} + f_{4d}|, \quad (2)$$

where f_i are the average atomic scattering amplitudes of the i sites. For the ordered Co₂MnSn with $q = 1$, $F(111) = 4|f_{\text{Mn}} - f_{\text{Sn}}|$, because the 4a and 4b sites are occupied by Mn and Sn atoms respectively, and the 4c and 4d sites are occupied by Co atoms. When $q = 0$, f_{4a} and f_{4b} are equal, so that $F(111) = 0$. The (220) reflection, on the other hand, is a principal lattice reflection so that the intensity is order independent. In this way the state of chemical disorder can be determined from the ratio of intensities of the Bragg peaks of (111) and (220) as shown in figure 2.

The bulk magnetization was measured using a superconducting quantum interference device (SQUID) magnetometer (Quantum Design, magnetic property measurement system) at a temperature of 5 K. The spontaneous magnetization was obtained by linear extrapolation of the isothermal M – H curves to zero field. ¹¹⁹Sn Mössbauer measurements were made at room temperature with a conventional absorption method with a constant-acceleration spectrometer using a Ca^{119m}SnO₃ source. A Pd foil was utilized as a filter to reduce the relative intensity of the 25.3 keV K x-ray of Sn from the source. The samples were mounted with the same thickness with respect to Sn (15 mg cm⁻²).

3. Experimental results

The XRD patterns of Co₂Mn_{1-x}Fe_xSn and Co₂Mn_{1-y}Cr_ySn are shown in figure 3. The XRD pattern of Co₂MnSn indicates that the sample we prepared has the typical $L2_1$ structure. The alloys of the Co_xMnSn system were investigated by Castelliz [8] and he reported that Co₂MnSn has Heusler structure with a lattice parameter of 5.977 Å. From the x-ray diffraction

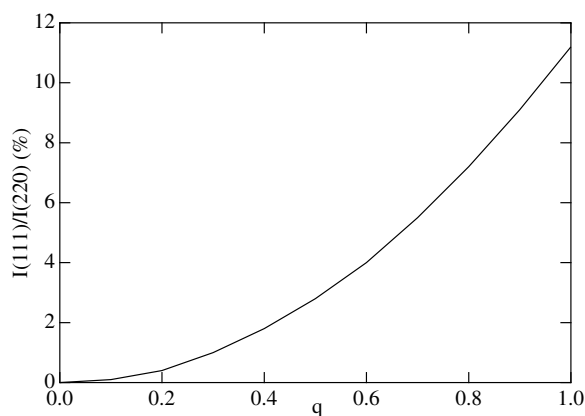


Figure 2. Calculated relative intensity of the superstructure Bragg reflection (111) plotted against the order parameter $q = 2p - 1$; here, p is the site occupation of Mn or Sn. $q = 1$ for the $L2_1$ -type structure and $q = 0$ for $B2$ -type structure.

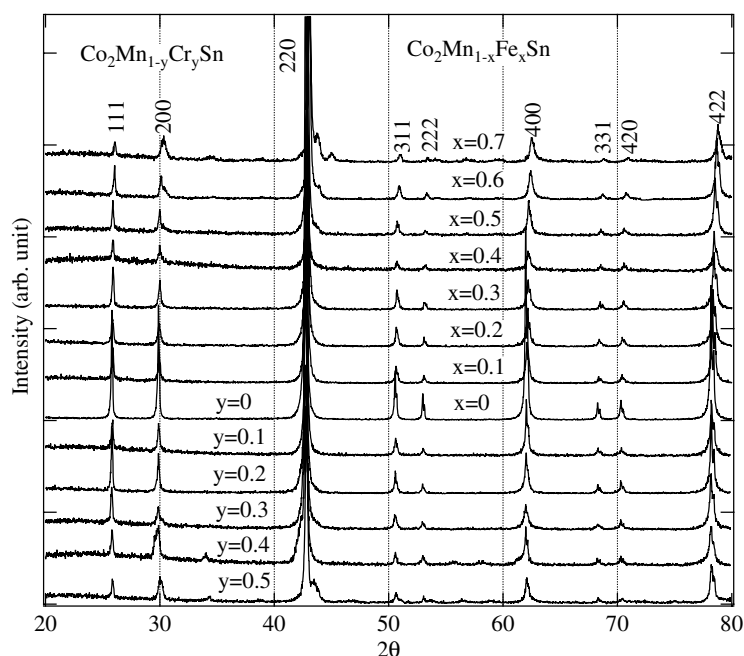


Figure 3. X-ray diffraction patterns of $\text{Co}_2\text{Mn}_{1-x}\text{Fe}_x\text{Sn}$ and $\text{Co}_2\text{Mn}_{1-y}\text{Cr}_y\text{Sn}$.

pattern in figure 3 the lattice constants of Co_2MnSn were estimated as $a = b = c = 5.98 \text{ \AA}$, $\alpha = \beta = \gamma = 90^\circ$ which are in good agreement with the reported values in [8].

XRD analyses indicated that the samples have a typical Heusler crystal structure in $\text{Co}_2\text{Mn}_{1-x}\text{Fe}_x\text{Sn}$ ($x \leq 0.5$) and in $\text{Co}_2\text{Mn}_{1-y}\text{Cr}_y\text{Sn}$ ($y \leq 0.3$). The lattice parameters of the alloys vary in Vegard's law as shown in figure 4. Because a Mn ion is larger than an Fe ion, but is smaller than a Cr ion, the Co_2MnSn lattice decreases for substitution with Fe and increases with Cr. For $\text{Co}_2\text{Mn}_{1-x}\text{Fe}_x\text{Sn}$ with $x > 0.5$, the samples contain a small amount of impurities such as Co_3Sn_2 and CoFe . For $\text{Co}_2\text{Mn}_{1-y}\text{Cr}_y\text{Sn}$ with $y \geq 0.4$, the samples contain

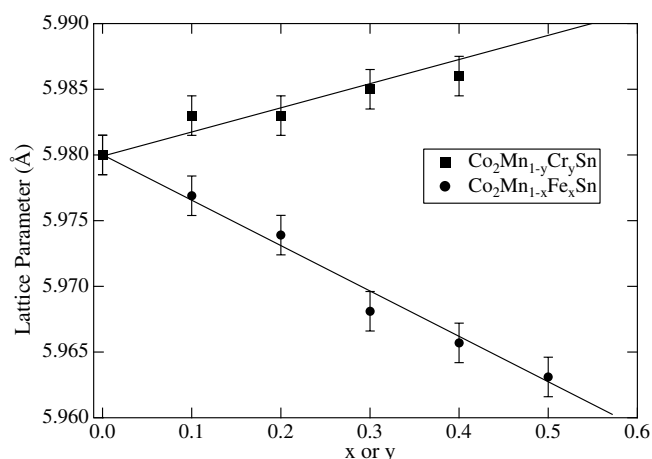


Figure 4. x or y dependence of the lattice parameter of the Heusler alloys Co₂Mn_{1-x}Fe_xSn and Co₂Mn_{1-y}Cr_ySn with $L2_1$ structures. The bars are the probable errors during measurements and calculations. The solid lines are guides to the eye.

a small amount of Co₃Sn₂ and CrCo. We find that the sample of Co₂MnSn after arc-melt has the order parameter q of ~ 0.9 whereas the sample of Co₂MnSn after arc-melt and annealing at 800 °C has the order parameter q of ~ 0.8 . We also find that almost all the samples in this research prepared by the arc-melting method have order parameters between 0.8 and 0.9. So we used the samples without annealing after arc-melt for magnetization and Mössbauer effect measurements in this research.

Magnetization curves of Co₂Mn_{1-x}Fe_xSn and Co₂Mn_{1-y}Cr_ySn measured at 5 K are shown in figure 5(a). The spontaneous magnetization at 5 K obtained from magnetization curves is plotted as a function of Fe or Cr concentration in figure 5(b). One can find that the spontaneous magnetization of Co₂MnSn is increased on substituting Mn with Fe and decreased on substituting Mn with Cr.

The ¹¹⁹Sn Mössbauer spectra obtained at room temperature are shown in figure 6. The spectrum of Co₂MnSn is almost the same as the spectra observed by several groups [10–16]. By computer fitting, we found that the spectra of Co₂MnSn consist of two sets of sextets reflecting some imperfection of the alloy from the ideal ordered structure. In this compound the Sn environment has cubic symmetry: hence, no electric quadrupole interaction is expected. The isomer shift relative to CaSnO₃ of the first (the major) component is 1.39 mm s⁻¹, and that of the second (minor) one is 1.46 mm s⁻¹. The hyperfine fields of the first and second components are $B_{\text{hf}}^{\text{1st}} = 9.82$ T and $B_{\text{hf}}^{\text{2nd}} = 4.52$ T, and the spectral weight-average of the B_{hf} of the two components is $\overline{B}_{\text{hf}} = 6.87$ T. $B_{\text{hf}}^{\text{1st}}$ is from Sn sites in perfectly ordered alloy. The sextets corresponding to $B_{\text{hf}}^{\text{2nd}}$ result from other local Sn environments.

4. Discussions

As mentioned by Galanakis *et al.*, the total spin magnetic moments M_t of the Co₂MnZ compounds follow the $M_t = Z_t - 24$ rule, where Z_t is the total number of valence electrons per unit formula [20]. This is the well known Slater–Pauling behaviour. In this picture the occupancy of the spin-down bands, which have an energy gap at the Fermi level, does not change and the number of added or subtracted electrons due to the change of Z_t is adjusted

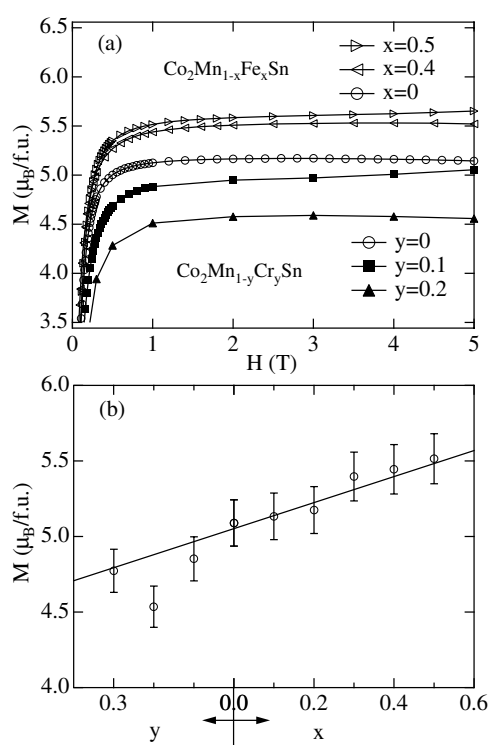


Figure 5. (a) Magnetization curves of $\text{Co}_2\text{Mn}_{1-x}\text{Fe}_x\text{Sn}$ and $\text{Co}_2\text{Mn}_{1-y}\text{Cr}_y\text{Sn}$ Heusler alloys at 5 K. (b) The x or y dependence of the spontaneous magnetic moments of $\text{Co}_2\text{Mn}_{1-x}\text{Fe}_x\text{Sn}$ and $\text{Co}_2\text{Mn}_{1-y}\text{Cr}_y\text{Sn}$. The bars are the possible error during the measurements and estimations. The solid line is the Slater–Pauling curves expected for half-metallic $\text{Co}_2\text{Mn}_{1-x}\text{Fe}_x\text{Sn}$ and $\text{Co}_2\text{Mn}_{1-y}\text{Cr}_y\text{Sn}$ systems (see details in text).

by the spin-up states only [20]. The alloys Co_2MnZ with 29 valence electrons when Z is a group IVB element, such as Si, Ge or Sn, have $\sim 5 \mu_B$ /formula, and the alloys containing the group IIIB element as Z , such as Co_2MnAl and Co_2MnGa , have $\sim 4 \mu_B$ /formula. Heusler alloys with 30 valence electrons have a spin moment with $6 \mu_B$ /formula. Galanakis *et al* substituted Sn in Co_2MnSn with Sb or As and calculated the total spin moment to be 5.620 or 5.782 μ_B /formula [20]. The Heusler alloys of Co_2FeSn and Co_2CrSn , if they existed, would have the magnetic moments of 6 and 4 μ_B , respectively, according to the Slater–Pauling behaviour. In the single-phase region of the systems of $\text{Co}_2\text{Mn}_{1-x}\text{Fe}_x\text{Sn}$ and $\text{Co}_2\text{Mn}_{1-y}\text{Cr}_y\text{Sn}$, we have observed that the magnetic moments increase when x increases and decrease as y increases (figure 5(b)), which is in good agreement with the Slater–Pauling behaviour in Heusler alloy.

The magnetic hyperfine fields at Sn nuclei in Co_2MnSn are estimated to be 9.9 T at 0 K by extrapolation of ^{117}Sn and ^{119}Sn NMR data [22]. Williams found that the major hyperfine field at ^{119}Sn was 10.7 T at 4.2 K by Mössbauer spectroscopy, and explained the results using prediction that the B_{hf} arises from the oscillating spin polarization induced in the conduction band by the magnetic moments localized on the Mn atoms [12]. In the present study, the B_{hf} value of the major component (9.8 T) agrees well with that reported by Williams [11]. The second component with low B_{hf} was attributed to a possible site disorder [11]. The Mn substitution affects the form of the Mössbauer spectra. The Mössbauer spectrum becomes

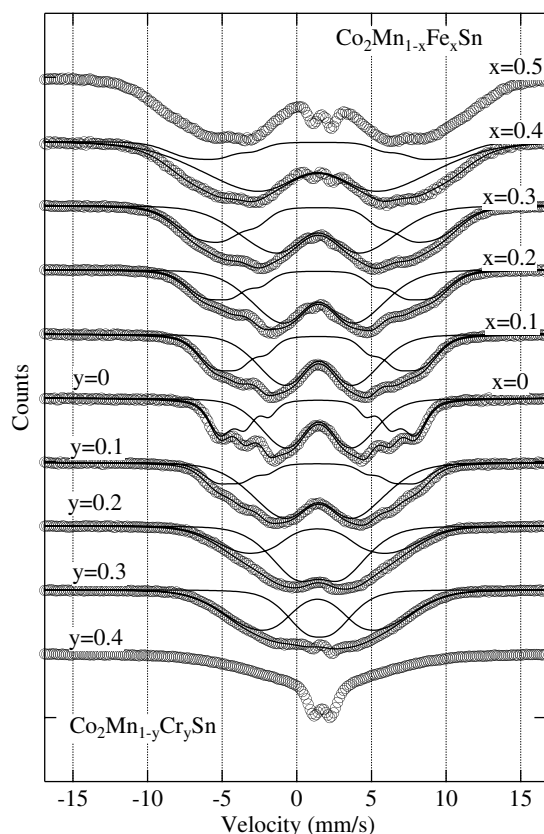


Figure 6. ¹¹⁹Sn Mössbauer absorption spectra at room temperature for Co₂Mn_{1-x}Fe_xSn and Co₂Mn_{1-y}Cr_ySn. Computer fits are shown by the solid lines.

broader when substituting Mn with Fe or Cr as shown in figure 6, which may be explained by the chemically disorder state in substituted samples. If the 4a site is partially occupied by Fe or Cr in Co₂MnSn, the ¹¹⁹Sn probe in the 4b site should sense this substitution by the change in conduction-electron density. Disorder in the 4a site or between 4a and 4b sites in Co₂Mn_{1-x}Fe_xSn and Co₂Mn_{1-y}Cr_ySn alloys results in a difference of magnetic environments around the Sn nuclei and causes a distribution of Sn hyperfine fields. In the measured Mössbauer spectra in figure 6, doublet lines were found for Co₂Mn_{1-x}Fe_xSn with $x \geq 0.2$ and Co₂Mn_{1-y}Cr_ySn with $y \geq 0.2$, whereas we did not find impurity peaks when $x \leq 0.5$ and $y \leq 0.3$ in the XRD patterns. These additional absorption lines may be from Sn atoms which are in a small percentage of non-Heusler phases.

The composition (x or y) dependences of the B_{hf} in the Sn nuclei obtained by least-square fitting of Mössbauer spectra and the value of isomer shift measured relative to the CaSnO₃ in Co₂Mn_{1-x}Fe_xSn and Co₂Mn_{1-y}Cr_ySn are give in figure 7. It was found that the value of B_{hf} at the Sn nuclei of Co₂MnSn increases by substitution with Fe and decreases by substitution with Cr. The isomer shift is almost unchanged on substituting Mn with Fe or Cr.

B_{hf} at a nonmagnetic impurity site in a ferromagnetic host is expressed as sum of partial contributions from neighbouring magnetic moments as

$$\overline{B}_{\text{hf}} = \sum_i \mu(r_i) p(r_i), \quad (3)$$

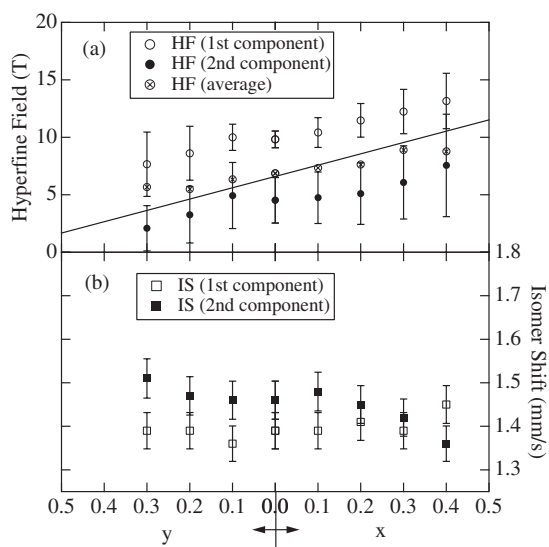


Figure 7. The composition (x or y) dependence of (a) the hyperfine field in the Sn nuclei obtained by computer fitting of Mössbauer spectra, and (b) the value of isomer shift relative to CaSnO_3 in $\text{Co}_2\text{Mn}_{1-x}\text{Fe}_x\text{Sn}$ and $\text{Co}_2\text{Mn}_{1-y}\text{Cr}_y\text{Sn}$. The bars in the B_{hf} (first component) and B_{hf} (second component) represent the width of the distribution and the bars in the δ are the errors of the least-square fittings. The straight line is a guide to the eye.

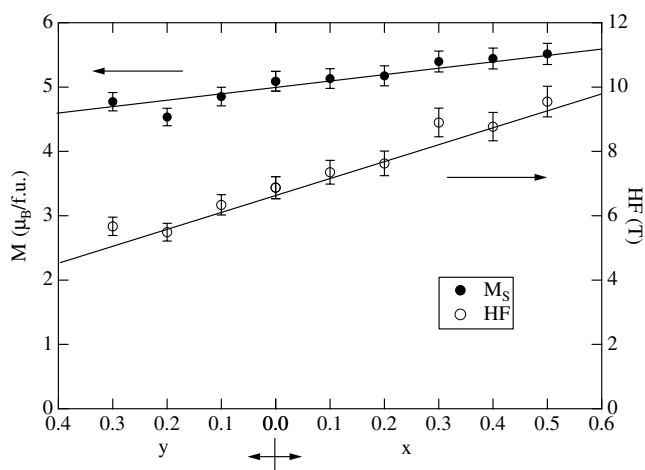


Figure 8. The composition (x or y) dependence of the average hyperfine field at the Sn nuclei and spontaneous magnetic moments in $\text{Co}_2\text{Mn}_{1-x}\text{Fe}_x\text{Sn}$ and $\text{Co}_2\text{Mn}_{1-y}\text{Cr}_y\text{Sn}$. The bars are the errors during computer fitting and the calculations. The upper straight line is the expected change from Slater Pauling behaviour; the lower line is a guide to the eye.

where μ is the magnetic moment of an atom located at r_i and $p(r_i)$ is the reduced partial contribution to the B_{hf} at the probed nucleus [15]. We have observed the composition dependence of B_{hf} in Sn nuclei and spontaneous magnetic moments in $\text{Co}_2\text{Mn}_{1-x}\text{Fe}_x\text{Sn}$ and $\text{Co}_2\text{Mn}_{1-y}\text{Cr}_y\text{Sn}$ as shown in figure 8. According to equation (3) and figure 8, we found that the Fe atoms would produce high B_{hf} on Sn when they substitute Mn in Co_2MnSn , and Cr atoms should produce low B_{hf} on Sn when they substitute Mn in Co_2MnSn .

5. Summary

Heusler alloys of pure Co₂MnSn and those with the Mn site substituted by Fe or Cr have been prepared by the arc melting method. The intermetallic compounds of Co₂Mn_{1-x}Fe_xSn and Co₂Mn_{1-y}Cr_ySn crystallize in a single phase with the L2₁-type structure at the concentration of $0 \leq x \leq 0.5$ and $0 \leq y \leq 0.3$. The synthesized samples have the order parameter between 0.8 and 0.9. In the range of a single phase, the substitution of Mn with Fe increases the spontaneous magnetic moments of Co₂MnSn, whereas the substitution of Mn with Cr decreases the magnetization. The trends of magnetic moments in Co₂Mn_{1-x}Fe_xSn and Co₂Mn_{1-y}Cr_ySn are in good agreement with Slater–Pauling behaviour. The Mössbauer spectra can be fitted by two components. The average B_{hf} at Sn nuclei increases by the substitution of Mn with Fe and decreases by the substitution of Mn with Cr. The distribution of B_{hf} studied by the Mössbauer effect is discussed in terms of the state of chemical ordering of the alloys.

Acknowledgments

The authors thank Professor T Ono for fruitful discussion during this work and acknowledge the support by the COE Project from the Ministry of Education, Culture, Sports, Science, and Technology of Japan.

References

- [1] Miyazaki T and Tezuka N 1995 Giant magnetic tunneling effect in Fe/Al₂O₃/Fe junction *J. Magn. Magn. Mater.* **139** L231–4
- [2] Moodera J S, Kinder L R, Wong T M and Meservey R 1995 Large magnetoresistance at room temperature in ferromagnetic thin film tunnel junctions *Phys. Rev. Lett.* **74** 3273–6
- [3] Prinz G A 1998 Magnetoelectronics *Science* **282** 1660–3
- [4] Julliere M 1975 Tunneling between ferromagnetic films *Phys. Lett. A* **54** 225–6
- [5] de Groot R A, Mueller F M, van Engen P G and Buschow K H J 1983 New class of materials: half-metallic ferromagnets *Phys. Rev. Lett.* **50** 2024
- [6] Inomata K, Okamura S, Goto R and Tezuka N 2003 Large tunneling magnetoresistance at room temperature using a Heusler alloy with B2 structure *Japan. J. Appl. Phys. B* **42** L419–22
- [7] Kubota H, Nakata J, Oogane M, Ando Y, Sakuma A and Miyazaki T 2004 Large magnetoresistance in magnetic tunnel junction using Co–Mn–Al full Heusler alloy *Japan. J. Appl. Phys. B* **43** L984–6
- [8] Castelliz L 1955 Beitrag zum ferromagnetismus von legierungen der Übergangsmetalle mit elementen der B-gruppe *Z. Metallk.* **46** 198–203
- [9] Webster P J 1971 Magnetic and chemical order in Heusler alloys containing cobalt and manganese *J. Phys. Chem. Solids* **32** 1221–31
- [10] Kuz'min R N, Ibrahimov N S and Zhdanov G S 1966 Mössbauer effect in Heusler alloys *Sov. Phys.—JETP* **23** 219
- [11] Williams J M 1968 Mössbauer effect in Heusler alloy Co₂MnSn *J. Phys.: Condens. Matter* **1** 473
- [12] Williams J M 1969 The sign of the internal field at ¹¹⁹Sn nuclei in Co₂MnSn *J. Phys.: Condens. Matter* **2** 2037
- [13] Dunlap R A, March R H and Stroink G 1981 Sn hyperfine field distributions in the Heusler alloys XMnSn and X₂MnSn *Can. J. Phys.* **59** 1577
- [14] Dunlap R A and Stroink G 1982 Magnetic and chemical ordering in Heusler system Co₂Mn_{1-x}Ti_xSn *Can. J. Phys.* **60** 909
- [15] Dunlap R A and Jones D F 1982 Mössbauer-effect study of Sn-impurity site hyperfine fields in the Heusler alloys Co₂MnZ (Z = Al, Ga, Si, Ge, Sn) *Phys. Rev. B* **26** 6013
- [16] Gavriluk A G, Stepanov G N and Irkaev S M 1995 Mössbauer study of $H_{\text{hpf}}^{\text{Sn}}$ in the Heusler alloy Co₂MnSn *J. Appl. Phys.* **77** 2648
- [17] Ishida S, Akazawa S, Kubo Y and Ishida J 1982 Band theory of Co₂MnSn, Co₂TiSn and Co₂TiAl *J. Phys. F: Met. Phys.* **12** 1111
- [18] Kübler J, Williams A R and Sommers C B 1983 Formation and coupling of magnetic moments in Heusler alloys *Phys. Rev. B* **28** 1745

-
- [19] Picozzi S, Continenza A and Freeman A J 2002 Co₂MnX (X = Si, Ge, Sn) Heusler compounds: An *ab initio* study of their structural, electronic, and magnetic properties at zero and elevated pressure *Phys. Rev. B* **66** 094421
- [20] Galanakis I, Dederichs P H and Papanikolaou N 2002 Slater–Pauling behavior and origin of the half-metallicity of the full-Heusler alloys *Phys. Rev. B* **66** 174429–1
- [21] Johnston G B and Hall E O 1968 Studies on the Heusler alloys—I. Cu₂MnAl and associated structures *J. Phys. Chem. Solids* **29** 193–200
- [22] Shinohara T and Watanabe H 1966 Nuclear magnetic resonance of cubic ferromagnetic compounds Co₂MnSn and CoMnSb *J. Appl. Phys.* **21** 1658